Kinetic model of ionization waves in a positive column at intermediate pressures in inert gases

Yu. B. Golubovskii,[1] V. A. Maiorov,[1] V. O. Nekutchaev,[1] J. Behnke,[2] and J. F. Behnke[2]
[1]*Faculty of Physics, St. Petersburg State University, Ulianovskaya ul., 1, 198904 Petrodvorets, St. Petersburg, Russia*
[2]*Institute for Physics, Ernst-Moritz-Arndt-University Greifswald, Domstrasse 10A, 17487 Greifswald, Germany*
(Received 22 August 2000; published 27 February 2001)

A kinetic model of ionization waves in the inert gas discharge is constructed, which is based on the simultaneous solution of the kinetic equation for electrons and the continuity equations for ions and excited atoms. The model corresponds to a range of intermediate pressures and small currents, when elastic collisions dominate in the electron energy balance and electron–electron collisions are negligibly small. A linear theory of ionization waves is constructed, growth rates and frequencies of wave disturbances able to propagate in plasma are found. It is shown that there is an upper bound to the existence of striations by pressure, as well as the lower bound by current. The self-consistent solution of the source system of equations is obtained, which describes a nonlinear wave. The profile of electric field and the electron distribution function in this field are calculated. The results of calculations are compared with the experimental data. The wavelengths obtained are essentially larger than the electron energy relaxation length. Such waves cannot be described within the limits of fluid models.

DOI: 10.1103/PhysRevE.63.036409 PACS number(s): 52.35.Mw, 52.25.Dg, 52.80.Hc

I. INTRODUCTION

It is well known that the positive column of a discharge in inert gases in a wide range of pressures and currents is found to be in a stratified state. The detailed diagram of discharge states is represented in Refs. [1,2]. The mechanisms of origin and propagation of waves depend essentially on the discharge conditions and can vary for different pressures and currents. In the present paper the discharge at small currents and intermediate pressures is studied, when the electron–electron collisions play an inessential role in the formation of the electron distribution function (EDF), and the energy balance is determined by elastic collisions. The calculations were performed for a neon discharge, in a range of currents $i<25$ mA and pressures $p=10$–40 Torr. At higher pressures striations are not observed. The mechanism of stratification at lower pressures is due to resonance effects, when the energy balance is determined by inelastic collisions. In this case the energy loss in elastic collisions is small and the electrons gain the excitation energy in a length L a little exceeding $U^{\mathrm{ex}}/(eE_0)$, (U^{ex} is the excitation threshold, E_0 is the mean electric field) with a subsequent inelastic collision. This length determines the spatial scale of field inhomogeneity, i.e., the striation length. This mechanism assumes that the energy relaxation length due to elastic collisions $\lambda_\varepsilon \sim \sqrt{(M/m)}\lambda$ (λ is the length of free flight of an electron, m and M are the masses of electron and atom, correspondingly) greatly exceeds the striation length, $\lambda_\varepsilon \gg L$. At low pressures the nonlocal nature of electron kinetics is clearly expressed, and the EDF is formed by the whole potential profile of a striation.

The opposite case is realized at intermediate pressures, when elastic collisions dominate in the energy balance, and, thus, the inequality $\lambda_\varepsilon < L$ is satisfied. The lower is the ratio λ_ε/L, the closer is the EDF to the local one. One can notice that, within the limits of local kinetics and fluid models, appearance of the waves with a length $L>\lambda_\varepsilon$ at intermediate pressures and small currents is impossible [3]. The principal reason is that, for waves with such a length, the disturbance of the ionization rate is in phase with the electric field, and the disturbance of the electron density is in antiphase.

Nevertheless, the existence of the striations at intermediate pressures and small currents can be understood in the framework of nonlocal kinetics, when spatial gradients are retained in the kinetic equation. For the first time such problem was discussed in Ref. [4], where the analytic solution of the kinetic equation was obtained in a spatially inhomogeneous field. Consideration of the effects of nonlocality yielded, that the EDF differs from the local one in a range of energies close to the excitation threshold. On the basis of the solution obtained, an example of ionization instability was studied, which was caused by phase shifts between the disturbances of ionization rate and electron density in a sinusoidally modulated field. On the basis of this mechanism in Refs. [5–7] the results of experiments were interpreted.

In Ref. [8] on the basis of the accurate numerical solution of the kinetic equation the EDF was obtained in a sinusoidally modulated field, its difference from local one was demonstrated, and the phase shifts between electric field, density, mean energy, and excitation rate were analyzed.

The aim of the present paper is the construction of the self-consistent one-dimensional model of ionization waves on the basis of a coupled solution of the nonlocal kinetic equation for electrons, and the continuity equation for ions. The linear analysis of steady-state solutions of these equations was performed, with the respect to the small wave disturbances. The dependence of growth rates and frequencies on wavelength was found from the dispersion relations for various discharge conditions. The nonlinear theory of ionization waves was constructed, which permitted us to compare the theoretical predictions with experiment [5,9].

II. BASIC EQUATIONS

The source equation for the description of the electron component in a plasma is the Boltzmann kinetic equation.

The temporal derivatives and radial gradients in this equation are negligible under the conditions discussed. Indeed, the energy relaxation length with the respect to elastic collisions at intermediate pressures appears to be considerably smaller than the tube radius. Thus, the radial electric field appears to be smaller than the axial one when the distance to the wall is more than λ_ε [10] and, consequently, the terms describing radial gradients in the kinetic equation appear to be small. The typical time of establishment of the isotropic part of the EDF has the value $\delta\tau\sim[(m/M)Q^{\mathrm{el}}Nv]^{-1}$ (Q^{el} is the cross section of elastic electron–atom collisions, N is the neutral atom density, v is the thermal electron velocity), which is considerably smaller than the period of a striation. Therefore, temporal derivatives in the kinetic equation are inessential and the EDF depends on the electric field in a current temporal point.

Taking these assumptions into account, the kinetic equation for a weakly anisotropic EDF, depending on the kinetic energy U and the axial coordinate x,

$$f(\vec{v},x)=\frac{1}{2\pi}\left(\frac{m}{2}\right)^{3/2}\left(f_0(U,x)+\frac{v_x}{v}f_1(U,x)\right), \tag{1}$$

reduces to the system of two equations for the isotropic and anisotropic parts of the EDF:

$$\begin{aligned}&-\frac{\partial}{\partial x}\left(\frac{U}{3}f_1(U,x)\right)+eE(x)\frac{\partial}{\partial U}\left(\frac{U}{3}f_1(U,x)\right)\\&\quad+\frac{\partial}{\partial U}\left(\frac{2m}{M}U^2NQ^{\mathrm{el}}(U)f_0(U,x)\right)\\&\quad=UNQ^{\mathrm{in}}(U)f_0(U,x)-(U+U^{\mathrm{ex}})NQ^{\mathrm{in}}(U+U^{\mathrm{ex}})\\&\qquad\times f_0(U+U^{\mathrm{ex}},x),\end{aligned} \tag{2}$$

$$\begin{aligned}&-\frac{\partial f_0(U,x)}{\partial x}+eE(x)\frac{\partial f_0(U,x)}{\partial U}\\&\quad=NQ^{\Sigma}(U)f_1(U,x),\end{aligned} \tag{3}$$

where Q^{in} is the cross section of inelastic electron–atom collisions, $Q^{\Sigma}=Q^{\mathrm{el}}+Q^{\mathrm{in}}\approx Q^{\mathrm{el}}$ is the total cross section of electron–atom collisions.

The EDF is normalized by the condition

$$n(x)=\int_0^\infty U^{1/2}f_0(U,x)dU, \tag{4}$$

where $n(x)$ is the electron density. The expression for the electron mean energy has the form

$$\overline{U}(x)=\frac{1}{n(x)}\int_0^\infty U^{3/2}f_0(U,x)dU, \tag{5}$$

and for the excitation rate

$$W(x)=\sqrt{\frac{2}{m}}\int_{U^{\mathrm{ex}}}^\infty UNQ^{\mathrm{in}}(U)f_0(U,x)dU. \tag{6}$$

The consequence of Eqs. (2) and (3) is the conservation of the electron current density,

$$j_e=\frac{1}{3}\sqrt{\frac{2}{m}}\int_0^\infty Uf_1(U,x)dU, \tag{7}$$

which is close to the total discharge current density.

The system (2) and (3) is more suitable for numerical solution in terms of the variables $\varepsilon=U+e\varphi(x)$ and x [$\varphi(x)$ is the potential of electric field],

$$\begin{aligned}&\frac{\partial}{\partial x}\left(\frac{U}{3NQ^{\Sigma}(U)}\frac{\partial f_0(\varepsilon,x)}{\partial x}\right)+\frac{\partial}{\partial\varepsilon}\left(\frac{2m}{M}U^2NQ^{\mathrm{el}}(U)f_0(\varepsilon,x)\right)\\&\quad=UNQ^{\mathrm{in}}(U)f_0(\varepsilon,x)-(U+U^{\mathrm{ex}})NQ^{\mathrm{in}}(U+U^{\mathrm{ex}})\\&\qquad\times f_0(\varepsilon+U^{\mathrm{ex}},x),\end{aligned} \tag{8}$$

$$f_1(U,x)=-\frac{1}{NQ^{\Sigma}(U)}\frac{\partial f_0(\varepsilon,x)}{\partial x}, \tag{9}$$

where the kinetic energy U is considered as a function of ε and x.

The ion distribution is described by the continuity equation taking account of ionization. The bulk recombination at small currents is negligibly small relative to the diffusion to the wall. The equation of axial ion distribution, under the approximation of ambipolar radial diffusion, has the form

$$\frac{\partial n(x,t)}{\partial t}-\frac{\partial}{\partial x}(b^in(x,t)E(x,t))=I(x,t)-\frac{n(x,t)}{\tau^i}, \tag{10}$$

where b^i is the ion mobility, τ^i is the time of ion ambipolar diffusion to the wall,

$$\frac{1}{\tau^i(x,t)}\approx\frac{2}{3}b^i\overline{U}(x,t)\left(\frac{2.4}{R}\right)^2, \tag{11}$$

$I(x,t)$ is the ionization rate. It is assumed in (10) that the direction of x axis coincides with the direction of electron movement and, thus, is opposite to the direction of an electric field.

Equations (8) and (10) form a self-consistent system, whose solution gives the profiles of electric field $E(x,t)$ and EDF $f_0(\varepsilon,x,t)$.

III. SOLUTION OF THE KINETIC EQUATION

For the first time the analytical solution of kinetic equations (2) and (3) in a range of electron energies below the excitation threshold was obtained in Ref. [4] in axially inhomogeneous positive fields. This solution is obtained by expansion with the respect to the small parameter λ_ε/L (L is the characteristic length of inhomogeneities, a wavelength in a spatially periodic field). The EDF was considered for both the thermal electrons $U\sim\overline{U}$ and the electrons with their energies close to the excitation threshold $U\sim U^{\mathrm{ex}}\gg\overline{U}$.

In a range of low energies the EDF differs weakly from

the local one, $f_0^0(U)$, and has the form

$$f_0(U,x)=f_0^0(U,E(x))+\frac{\lambda_\varepsilon}{L}f_0^1(U,E(x))\frac{L}{E_0}\frac{dE(x)}{dx}. \tag{12}$$

Dependence (12) is convenient, because the EDF and, therefore, its integrals, appear to be the functions of a local field in the point x and its gradient in this point. This allows one to introduce the left part of Eq. (10) as the differential operator of $E(x,t)$, that simplifies greatly the calculation of a self-consistent electric field.

In the energy range close to the excitation threshold the EDF significantly differs from the local one. In this case the solution has the form [4]

$$f_0(U,x)=C(e\varphi(x)+2U)\times\tilde{n}(e\varphi(x)+2U)\sqrt{\frac{\tilde{E}(e\varphi(x))}{\tilde{E}(e\varphi(x)+2U)}}\times\exp\left[-\int_0^U\frac{6m}{M}\frac{N^2Q^2(U')U'dU'}{[e\tilde{E}(e\varphi(x)+2U-2U')]^2}\right]. \tag{13}$$

In this expression $\tilde{n}$ and $\tilde{E}$ are the functions of a potential and are determined by relations $\tilde{n}(e\varphi(x))\equiv n(x)$ and $\tilde{E}(e\varphi(x))\equiv E(x)$.

As it is seen from (13), the EDF is determined by the values of electric field $\tilde{E}$ in the interval from $e\varphi(x)$ to $e\varphi(x)+2U$. The drawback of the solution (13) is the impossibility of the normalization on a constant current density, that makes the calculation of the absolute values of the excitation rates difficult. A possible choice of the normalization function $C(e\varphi(x)+2U)\cdot\tilde{n}(e\varphi(x)+2U)$ can be the equality of a solution (13) to the local EDF in the limit $U\to 0$. Thus, construction of an analytical theory is possible when using the EDFs (12) and (13). A similar problem was considered in Ref. [7] under some restrictions.

In the present paper the theory is based on the numerical solution of the kinetic equation (8) by the method, described in detail in Ref. [11]. The approximation (12) was used for calculation of the electron density.

It can be interesting to compare accurate and approximate calculations of such macroscopic parameters as the electron density and excitation rate. The results of calculations in neon, using the cross sections $Q^{\rm el}(U)$ and $Q^{\rm in}(U)$ from Ref. [12], are shown in Fig. 1. It is seen from the figure, that the electron density has a small phase shift with respect to the local one. This phase shift is well described by the approximate analytical solution (12). The essential difference between accurate and local solutions can be seen for the excitation rate, in both the absolute value and the phase shift. The approximate solution differs from the accurate one by a factor of 1.5 and gives a larger phase shift. Thus, it is possible to use analytical solutions (12) and (13) for a qualitative analysis. It is preferable to use a numerical solution for comparison with experiment.

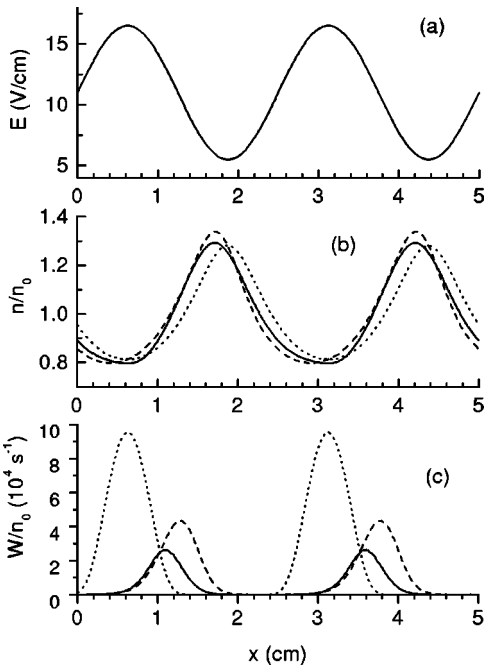

FIG. 1. The comparison of the electron density (b) and excitation rate (c) obtained from the local EDF (dotted curve), from the analytical solution (12) and (13) (dashed line), and from the numerically calculated EDF (solid curve), in the electric field (a) at the pressure $p=25$ Torr.

IV. MECHANISMS OF IONIZATION

The main processes of ionization at intermediate pressures are the stepwise ionization and the associative ionization from highly excited states located close to the ionization potential. The frequency of these processes can be expressed in terms of the EDF and the densities of metastable or resonance atoms, which are involved in the ionization processes,

$$I(x)=\sqrt{\frac{2}{m}}\sum_k N_k\left[\int_{U_k^{\rm ion}}^\infty UQ_k^{\rm ion}(U)f_0(U,x)dU+\int_{U_k^{\rm in}}^\infty UQ_k^{\rm in}(U)f_0(U,x)dU\right]\equiv\sum_k N_k\nu_k^{\rm ion}, \tag{14}$$

where $Q_k^{\rm ion}(U)$ and $U_k^{\rm ion}$ are the cross section and the potential of the stepwise ionization from the state k, $Q_k^{\rm in}(U)$ and $U_k^{\rm in}$ are the cross section of production of a molecular ion and the corresponding potential. The role of direct ionization under the conditions discussed is negligibly small.

The source states for stepwise ionization in inert gases are the closely located resonance and metastable levels (in particular, $2p^53s$ in neon). The balance equations for the densities of these states were discussed in detail in Ref. [13] for low pressures (units of Torr) in neon. At intermediate pressures, the processes of intermixing of the states $^3P_{0,1,2}$ due to collisions with atoms and electrons take place efficiently.

This causes the ratio of these state densities to be constant along a striation, which allows us to unify these states into one effective state, the source for the ionization processes. The weakly populated level $^1P_1$ takes little part in the process of ionization, but the transition to this level from the states $^3P_{0,1,2}$ with subsequent escape of resonance radiation, can be the effective channel of the destruction of these states.

A diffusion equation taking account of the processes of excitation and destruction describes the kth metastable state density rather well,

$$\frac{\partial N_k}{\partial t} = W_k + D_k^m \frac{\partial^2 N_k}{\partial x^2} - N_k \left(\frac{1}{\tau_k^m} + \nu_k^{\mathrm{ion}} \right) + \sum_{l \neq k} (N_l Z_{lk} - N_k Z_{kl}), \tag{15}$$

where W_k is the excitation rate of kth state, D_k^m is the diffusion coefficient, $1/\tau_k^m \approx D_k^m (2.4/R)^2$ is the lifetime due to processes of diffusion to the wall, ν_k^{ion} is the frequency of stepwise ionization from the kth state, Z_{kl} is the total transition constant from the state k to the state l of a system of resonance and metastable states due to collisional and radiative processes.

The densities of resonance states are described by the Holstein–Biberman integral equation [14,15], which generally does not reduce to the diffusion equation because of the divergence of the length of photon free flight. Nevertheless, in a one-dimensional model of a cylindrical discharge one can introduce the coefficient of axial diffusion $D^r \sim R^2 \cdot A^{\mathrm{eff}}$, where A^{eff} is the effective probability of a resonance radiation escape [$A^{\mathrm{eff}} \approx (A/\sqrt{\pi k_0 R})$ for the Lorentzian profile of a spectral line, k_0 is the absorption coefficient in the center of line profile, A is the probability of spontaneous emission]. This approximation reduces the integral balance equation of a resonance state to the equation similar to (15), changing D_k^m to D_k^r and $1/\tau_k^m$ to A_k^{eff}. Thus, the system of equations (15) with different k describes the densities of all the metastable and resonance states uniformly.

The system (15) is valid when radial distributions of metastable and resonance atoms are close to fundamental modes of corresponding operators. When these radial distributions differ from fundamental modes significantly, consideration of the higher modes is necessary. Under the conditions discussed, a diffuse discharge is observed experimentally and, therefore, one can assume (15) to be valid.

The assumption of the constant ratio of densities N_k along a striation allows us to introduce a density of kth state in the form of $N_k(x,t) = \alpha_k N^*(x,t)$, where N^* is the total density of all the metastable and resonance states, and $\Sigma \alpha_k = 1$. Substituting these expressions into the system (15) and summing over k yields the equation for the total density,

$$\frac{\partial N^*}{\partial t} = W + D \frac{\partial^2 N^*}{\partial x^2} - N^* \left(\frac{1}{\tau} + \nu^{\mathrm{ion}} \right), \tag{16}$$

where W is the total excitation rate, calculated from the EDF using Eq. (6), and the other coefficients have the form

$$D = \sum_k \alpha_k D_k, \quad \frac{1}{\tau} = \sum_k \frac{\alpha_k}{\tau_k}, \quad \nu^{\mathrm{ion}} = \sum_k \alpha_k \nu_k^{\mathrm{ion}}. \tag{17}$$

Equation (16) allows one to obtain the rate of stepwise and associative ionization, $I(x,t) = N^*(x,t)\,\nu^{\mathrm{ion}}(x,t)$, which is used in Eq. (10).

V. LINEAR THEORY OF THE IONIZATION WAVES

The system (8), (10), (16) has a steady-state solution, which corresponds to the nonstratified positive column of a discharge. Indeed, the kinetic equation in the form (2), (3) reduces in this case to the equation for a local EDF, which depends on U and E_0/N. The local EDF as well as its integrals, are normalized at the electron density. The electron density is determined by the given discharge current,

$$n_0 = \frac{j}{b^e E_0} = \eta \frac{i}{R^2 b^e E_0}, \tag{18}$$

where b^e is the electron mobility, calculated from the EDF, i is the discharge current, η is a coefficient determined by a radial distribution of electron density, which has an order of unit. Under the approximation used, the radial distribution of charged particles is described by a Bessel function, and $\eta \approx 1.45$. The system (10), (16) appears to be

$$N_0^* \nu_0^{\mathrm{ion}} = \frac{n_0}{\tau_0^i}, \tag{19}$$

$$W_0 = N_0^* \left(\frac{1}{\tau} + \nu_0^{\mathrm{ion}} \right). \tag{20}$$

This system is nonlinear for the electron density and allows us to determine the reduced values of internal discharge parameters E_0/p and $n_0 R$ in dependence on external parameters pR and i/R. Thus, this system, together with the corresponding kinetic equation, describes homogeneous discharge completely.

The homogeneous state of a discharge appears to be unstable under the conditions discussed. The linearization of the system (8), (10), (16) with the respect for small complex disturbances, proportional to $\exp i(kx - \omega t)$, is used to study the properties of ionization waves. The wave vector k is assumed to be real, that is, the temporal development of spatially periodic disturbances is studied.

The numerical solution of Eq. (8) gives the EDF in a disturbed field $E(x) = E_0 + E_1 \cos(kx)$ (where E_1 is real). The small complex additions to the integrals of the EDF are obtained as magnitudes of their first Fourier mode. The quasistationarity of the kinetic equation permits us to replace kx by $kx - \omega t$.

Linearization of Eqs. (10) and (16) yields the following system:

$$-i\omega n_1 - ikb^i(n_0E_1 + n_1E_0) = N_0^*\nu_1^{\text{ion}} + N_1^*\nu_0^{\text{ion}} - \frac{n_0}{\tau_1^i} - \frac{n_1}{\tau_0^i}, \tag{21}$$

$$-i\omega N_1^* + k^2DN_1^* = W_1 - N_0^*\nu_1^{\text{ion}} - N_1^*\nu_0^{\text{ion}} - \frac{N_0^*}{\tau_1^i} - \frac{N_1^*}{\tau_0^i}, \tag{22}$$

where the lower index 0 corresponds to the stationary values, and 1 corresponds to the small additions. This system determines the frequency ω' and growth rate ω'' as a function of the wave vector k or, correspondingly, wavelength $L = 2\pi/k$. The system (21), (22) reduces to a quadratic equation for ω. The positive value of frequency ω' corresponds to propagation of the wave along the x axis, i.e., from cathode to anode. This solution has a great negative growth rate and, consequently, damps in time, for any values of external parameters. The positive growth rate corresponds to the negative value of frequency, i.e., the wave propagates from anode to cathode.

Linear analysis permits us to obtain the dependence of ω' and ω'' on k or, correspondingly, on L. Consideration of these dependences for various pressures and currents gives the instability domain, as well as the range of wavelengths and frequencies able to propagate in plasma. Generally, under the conditions discussed the waves appear to be strongly nonlinear, and as the instability develops, the parameters of a wave can change significantly. Consequently, the linear analysis, in spite of the accurate numerical realization, can give only a qualitative picture of excitation and propagation of the ionization waves. The wavelength related to the maximum of growth rate, also may not correspond to the observed wavelength. Nevertheless, the dependence of the maximum of growth rate on external parameters can be the same as for the length of an established wave.

VI. NONLINEAR THEORY OF THE IONIZATION WAVES

Analysis of the stationary solution of the system (8), (10), (16) for stability, described in the preceding section, allows us to obtain a range of lengths and frequencies of the waves able to propagate. In the present section the method of solution of this system is described, which permits us to determine the amplitude and profile of a wave, as well as the value of wavelength and frequency. The wave moving in space and time is described by a periodic function of one variable $\tilde{x} = x - vt$, where $v = L\nu$ is the phase velocity of a striation. Consequently, temporal derivatives in Eqs. (10), (16) are to be replaced by $-v(\partial/\partial\tilde{x})$.

The scheme of solution of the system (8), (10), (16) is shown in Fig. 2. As the source data for the problem one has to take the values of the discharge current i, pressure p, and the tube radius r. The method consists of two stages. In the first stage, the self-consistent profiles of electric field and EDF are calculating under an externally fixed length and frequency of a wave. In the next stage, the wavelength and frequency are obtained.

Let us fix the length and frequency of a wave. Equation

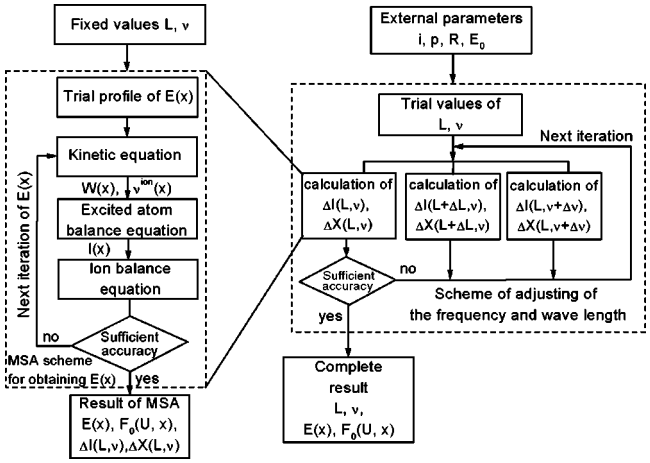

FIG. 2. The scheme of the self-consistent solution of Eqs. (8), (10), (16).

(8) gives the EDF and, therefore, electron density, excitation, and ionization rates, in a fixed electric field. The field is determined by the ion balance equation (10). The most obvious method of solution of such a system appears to be the method of successive approximations (MSA). In an arbitrary electric field the EDF is calculated, its integrals are substituted into Eq. (10), and a new iteration of the field is obtained from this equation.

The convergence of the MSA is caused by using expressions for the electron density and mean energy, which are functions of the electric field and its gradient, taking account of Eq. (12). These expressions have the form

$$n(x) = n_0(E(x)) + n_1(E(x))\frac{dE}{dx}, \qquad \overline{U}(x) = \overline{U}_0(E(x)) + \overline{U}_1(E(x))\frac{dE}{dx}. \tag{23}$$

The ionization term in Eq. (10) is determined by Eq. (16). A profile of excitation rate in this equation depends weakly on an electric field profile and has the form of a narrow Gaussian peak. Thus, varying the field profile weakly affects the profile of ionization rate. Taking Eq. (23) into account, Eq. (10) is the nonlinear differential equation for the electric field. The ionization rate plays the role of free term.

Thus, the MSA with the fixed wavelength and frequency is the following. An arbitrary field (for example, sinusoidally modulated one) with the period L is substituted into the kinetic equation (8). The EDF is calculated numerically, which gives the dependence of the excitation rate and the stepwise ionization frequency on x. These functions are used in the balance equation for excited atoms (16), whose solution is the density of excited atoms $N^*(x)$. This equation is replaced by a system of finite difference linear equations, taking the boundary conditions (periodicity and continuous differentiality) into account. Further, we obtain the ionization profile used in the ion balance equation (10). As the solution of this equation should be periodic, the integral ion balance must be satisfied,

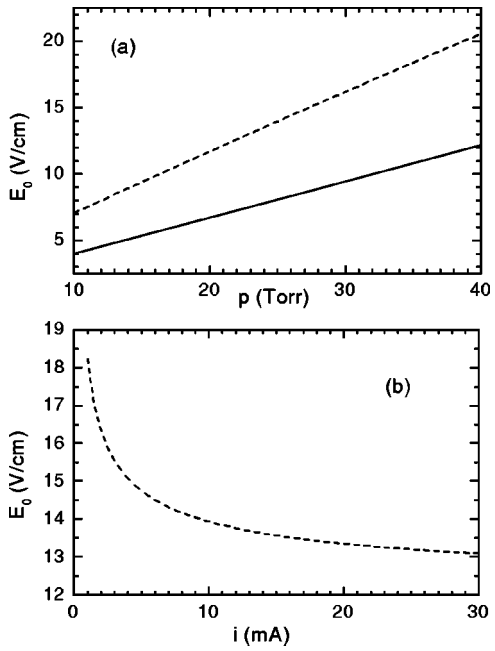

FIG. 3. The dependences of the mean electric field E_0 on pressure (a) at the current $i=10$ mA and on current (b) at the pressure $p=25$ Torr, calculated for the homogeneous column (dashed curve) and experimentally measured (solid curve). The tube radius R is 1.4 cm.

$$\int_0^L I(x)dx = \int_0^L \frac{n(x)}{\tau^i(x)}dx. \tag{24}$$

In this stage, Eq. (24) is supposed to be satisfied, i.e., the preliminary normalization of $I(x)$ is carried out. Equation (10) was solved by a Runge–Kutta method, and the condition of periodicity was satisfied by varying the initial conditions. This solution is the next field iteration. The peculiarity of this method is the indefinity of the mean field in the discharge E_0. This field affects the integral ion balance (24). It is necessary to keep this field constant for all the iterations.

The process of calculation of the self-consistent electric field converges rapidly. After five iterations, the successive approximations are very close, but a constant phase shift occurs between successive iterations. This phase shift is caused by disadjusting of the wavelength and frequency after a transition to the variable $x-vt$, and has to be determined.

In the present method, three undefined parameters of a solution appear: wavelength L, frequency ν, and mean electric field E_0. One of the equations determining these parameters is Eq. (24). The other condition is the adjusting of the phase shift of successive approximations. Consequently, one parameter remains indefinite. It follows from this, a continuous spectrum of waves can propagate in the studied system. The indefinity can be removed by taking the discharge boundaries into consideration, or by externally fixing one of the parameters, for example, from the experimental data. In particular, in the present paper the calculations were carried out with a fixed mean electric field, experimentally measured in Ref. [9]. The field is shown in Fig. 3(a) (solid curve). Thus, it is necessary to calculate two parameters, L and ν, to obtain a complete solution.

The method of adjusting of the wavelength and frequency is the following. When obtaining the profile of electric field in fixed L and ν, the discrepancy of the integral ion balance

$$\Delta I(L,\nu) = \ln\int_0^L I(x)dx - \ln\int_0^L \frac{n(x)}{\tau^i(x)}dx \tag{25}$$

together with the phase shift of the successive iterations $\Delta X(L,\nu)$ is calculated. To get a complete solution, it is necessary to satisfy the conditions $\Delta I(L,\nu)=0$ and $\Delta X(L,\nu)=0$, that is, to solve a system of two equations for two variables. A peculiarity of this system is a great computing time to calculate the values of functions ΔI and ΔX (it is necessary to pass all the first stage of a solution to calculate the value) and the rather large inaccuracy of this value. Considering this, as well as the closeness of this system to a linear one, the modified Newton method was chosen to solve it.

VII. APPLICATION OF THE THEORY TO THE NEON DISCHARGE

In the present section the application of the above stated theory to the neon discharge is discussed and the comparison between the calculation and the experimental data is performed.

A. Constants of elementary processes

Equation (16) contains the relative densities α_k. An approximate calculation of these coefficients can be performed by solving the system (15) in an homogeneous discharge with the help of a local EDF and the corresponding constants of intermixing. One can also use the relative densities, experimentally measured in Ref. [16].

The principal role in the processes of diffusion and destruction under the conditions discussed is played by the resonance state 3^3P_1. The effective lifetime of resonance state is determined by an absorption coefficient in the center of a spectral line. These lifetimes are estimated as $A^{\rm eff}\sim 10^{-4}$ s for 3^3P_1 and $A^{\rm eff}\sim 10^{-6}$ s for 3^1P_1 [13]. They do not depend on pressure for a Lorentzian profile. Thus, one can also estimate the diffusion coefficients of resonance atoms. The validity of the estimation should be checked by comparison with experiment. In the present paper the mean lifetime of excited atoms was chosen to be equal $\tau^{-1}=2\times 10^3$ s^{-1}, and the corresponding diffusion coefficient $D=(1/\tau)(R/2.4)^2$. These values are in accordance with both the above stated lifetimes of resonance atoms and the experimental data for ionization waves. For comparison with the experimental data [5,9], the tube radius R was chosen to be equal 1.4 cm.

The cross sections of stepwise and associative ionization used in the present paper, were taken from Ref. [17]. The value of the reduced ion mobility in neon is assumed to be independent of field and given by $b^i\cdot p = 3.2\times 10^3$ cm^2 V^{-1} s^{-1} Torr [18].

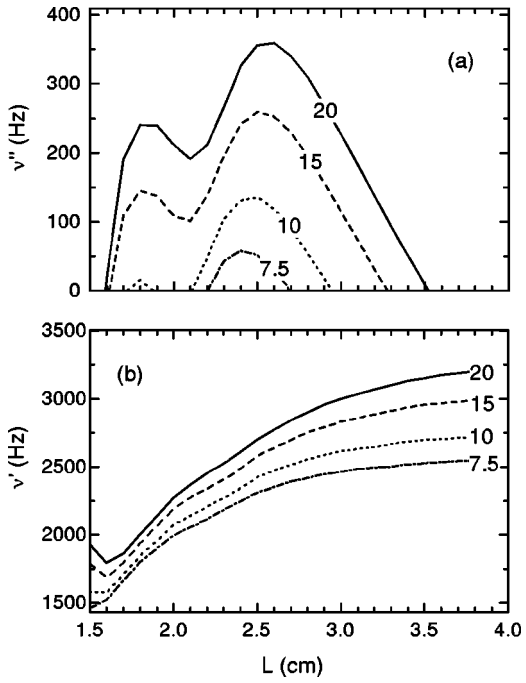

FIG. 4. The dependences of the growth rate ν'' (a) and frequency $|\nu'|$ (b) on the wavelength at $p=25$ Torr. $i=20$ mA (solid curve); $i=15$ mA (dashed curve); $i=10$ mA (dotted curve); $i=7.5$ mA (dashed–dotted curve).

B. Results of the linear theory

The solution of the system (19), (20) for a stationary discharge with the help of a local EDF yields the dependence of the electric field E_0 on external parameters. The dependence of the electric field on pressure is shown in Fig. 3(a) (dashed curve) in comparison with the experimental data [9], obtained in a stratified discharge (solid curve). It can be seen that the calculated values of the electric field are larger than the experimental values. This demonstrates an essential role of nonlinear waves in the formation of a discharge. The dependence of the calculated field on discharge current is shown in Fig. 3(b).

Two solutions of the system (21), (22) correspond to the positive and negative values of frequency. A positive value ω' corresponds to a large negative growth rate ω'' for all the external parameters. A limited range of wave lengths with a positive growth rate, is found to be for negative values of ω'. Consequently, the wave propagates from anode to cathode in agreement with the experimental data.

In Fig. 4 the dependences of the growth rate $\nu'' \equiv \omega''/(2\pi)$ (a) and frequency ν' (b) on the wavelength are represented for different currents and $p=25$ Torr. In this figure one can see the complex behavior of the growth rate, which has two maxima. The range of positive growth rate is limited both by short and long wavelengths. Presence of the lower bound is due to the axial diffusion. When the length increases, the phase shift between the ionization and density increases too and localization of the EDF occurs, that is the reason for the presence of an upper bound. The growth of the frequency with the current is seen in Fig. 4(b), which is in agreement with the experimental data [9]. In Refs. [1,2] the presence of a lower bound by current was shown, which is also described by the present theory.

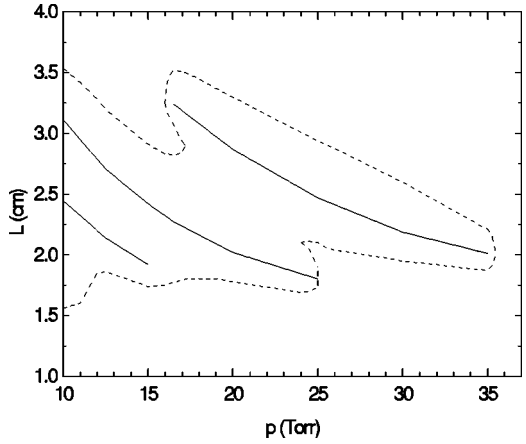

FIG. 5. The dependence of wavelengths in the maximum of the growth rate on pressure (solid curve). A bound of stability (dashed curve). $i=10$ mA.

The dependence of the growth rate for different pressures is more complex. In Fig. 5 the wavelengths corresponding to the maxima of the growth rate are represented as functions of the pressure (solid curves), at the current $i=10$ mA. The dashed curve denotes the limit of the region, where the growth rate is positive. One can see an upper bound for the existence of striations by pressure, which was also observed in experiment [1,2]. This is because nonlocality occurs only when wavelengths are small. At small lengths the effect of the axial transport of the resonance radiation, which is described in the present paper by the axial diffusion, damps the wave. The coefficient of the axial diffusion of excited atoms due to the resonance radiation transport is independent on pressure and damps the waves with their lengths $L<1.5$ cm, that can be seen in Fig. 5.

The length corresponding to the maximum of the growth rate in Fig. 5 decreases as the pressure grows. This is in qualitative agreement with the results of experiment [9], where a similar behavior of the striation length was observed. The comparison of this length with that calculated by nonlinear theory and measured in experiment is performed in Fig. 6.

Thus, analysis of a stationary solution for stability shows the presence of a limited domain of instability. The form of this domain and its dependence on various discharge parameters is in qualitative agreement with experiment.

C. Results of the nonlinear theory

One of the parameters in the nonlinear solution remains indefinite. The experimental values of the mean field dependence on pressure, which are shown in Fig. 3(b) (solid curve) at the current $i=10$ mA, were used in the calculations. Thus, the calculation of the wave parameters was carried out for different pressures.

The self-consistent values of wavelength are represented in Fig. 6(a) (solid curve). The circles denote the experimental values of the length of a wave stabilized by a frequency 1200 Hz [9]. The natural striations are mostly irregular under the

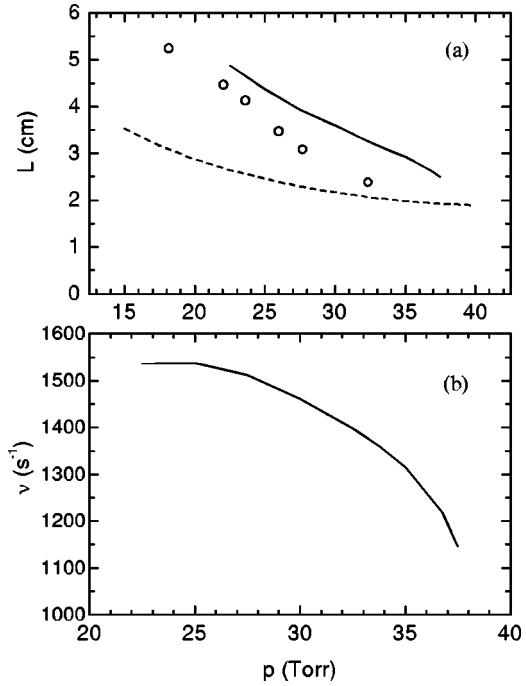

FIG. 6. The parameters of an ionization wave in dependence on pressure at $i=10$ mA. (a) The wavelength: nonlinear theory (solid curve); the length corresponding to the maximum of increment in the linear theory (dashed curve); experimental data under the stabilization frequency $\nu=1200$ Hz (points). (b) the calculated frequency of the nonlinear wave.

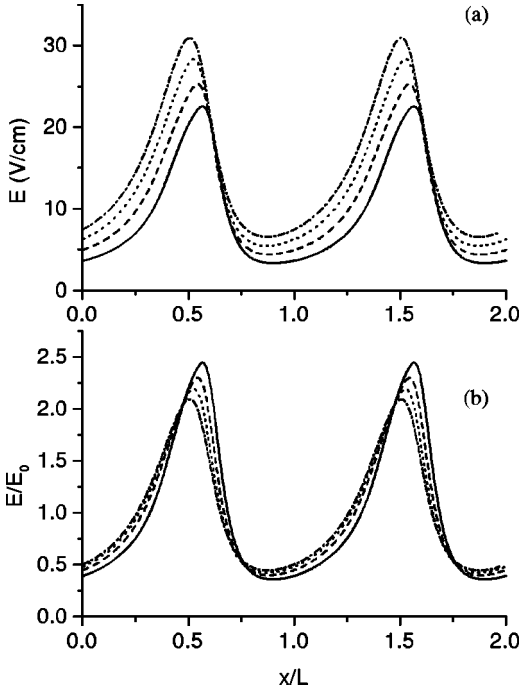

FIG. 7. The profiles of the electric field at different pressures and $i=10$ mA: (a) absolute values; (b) normalized. $p=25$ Torr (solid curve); 30 Torr (dashed curve); 35 Torr (dotted curve); 40 Torr (dashed–dotted curve).

conditions discussed. The decrease of the wavelength as the pressure increases is seen in the figure, in both theory and experiment. Taking into account the inaccuracy of the constants for the resonance radiation trapping and the model approximations, one can consider the agreement to be satisfactory. The dashed curve denotes the length corresponding to the maximum of the growth rate in the linear theory. The difference between this curve and experimental points is more significant. It is interesting to note that, both the calculated and experimental wavelengths generally are outside the instability domain, which is shown in Fig. 5. There is no contradiction, because the wave is strongly nonlinear and the established regime can strongly differ from an initial disturbance by its parameters.

The frequency calculated in the nonlinear theory is represented in Fig. 6(b). As the pressure grows, the frequency is approximately constant, and further it decreases. This circumstance causes the presence of a singularity in the ion continuity equation (10), when the ion drift velocity reaches the phase velocity of a striation. Indeed, the estimation of two terms in the left part of Eq. (10) gives that, the first term, corresponding to the phase velocity of a striation, is greater than the second one, which corresponds to the ion drift velocity. As the pressure grows, both the frequency and wavelength decrease, whereas the second term weakly depends on pressure. This singularity can be the reason for the irregularity of striations as the pressure increases. Indeed, the growth of irregularities with pressure was observed in experiment [6]. Further, as the current increases, the electric field and, consequently, the drift velocity, decrease and, thus, the singularity should occur at higher pressures. The experimental data [6] show that, at larger currents, the upper boundary of the regularity of striations shifts to the higher pressures.

The profiles of electric field at different pressures are represented in Fig. 7. The electric field in a nonlinear ionization wave differs strongly from a sinusoidally modulated one. Graphs of the normalized profiles (b) show a slight decrease in the field modulation as the pressure grows. The upper pressure bound for the existence of striations was 35 Torr in

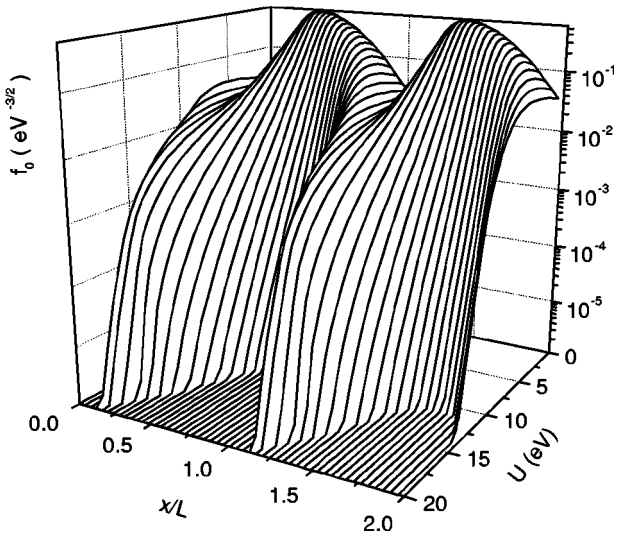

FIG. 8. The graph of the EDF calculated in the self-consistent electric field ($p=25$ Torr, $i=10$ mA).

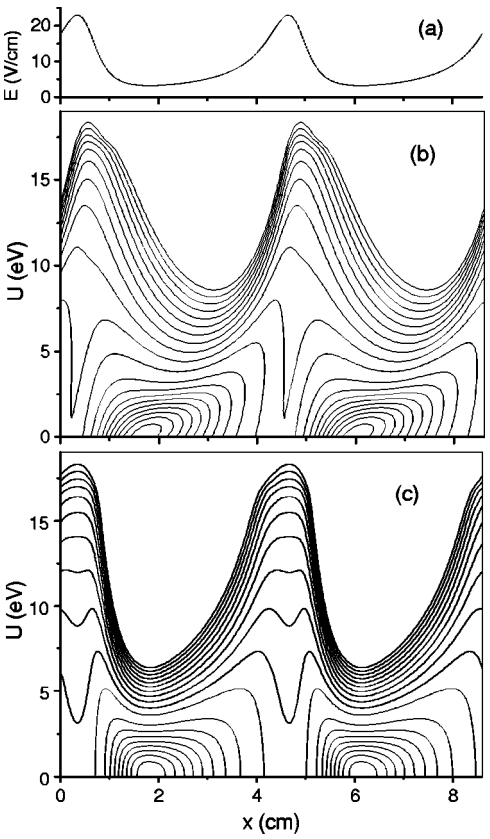

FIG. 9. (a) Self-consistent electric field at $p=25$ Torr, $i=10$ mA; (b) contour graph of the EDF; (c) contour graph of the local EDF in this field.

the linear analysis (Fig. 5). A nonlinear solution exists also at higher pressures, that can be caused by an essential decrease of the mean electric field as the wave disturbance develops (the magnitude of the ionization rate strongly depends on electric field and is very sensitive to its modulation). The experimental value of this limit is $pR \approx 60$ Torr cm [1].

A complete solution of the problem allows one to obtain the EDF in the self-consistent field and to construct a picture of the excitation and ionization processes occurring in a striation. In Fig. 8 the three-dimensional graph of the EDF is shown. In Figs. 9(b) and 9(c) the contour graphs of the nonlocal and local EDF are represented, which are correlated with the electric field (a). The nonlocality of the EDF is distinctly seen when comparing Figs. 9(b) and 9(c) and is caused by the diffusion of electrons in the coordinate space.

In Fig. 10 the electric field $E(x)$ (a), calculated profiles of the excitation rate of the metastable and resonance atoms $W(x)$ (b), their density $N^*(x)$ (c), ionization rate $I(x)$ (d), and electron density $n(x)$ (e), are shown. It is seen from this figure that, the sources of excited atoms are localized in a narrow domain, approximately $0.1L$ in width, and the resonance radiation transport causes the essential broadening of the profile of the excited atom density. The profile of the stepwise ionization rate is also broad. The maximum of the ionization rate is shifted in the cathode direction with respect to the density maximum for a value of approximately $L/4$, that stimulates the propagation of ionization waves.

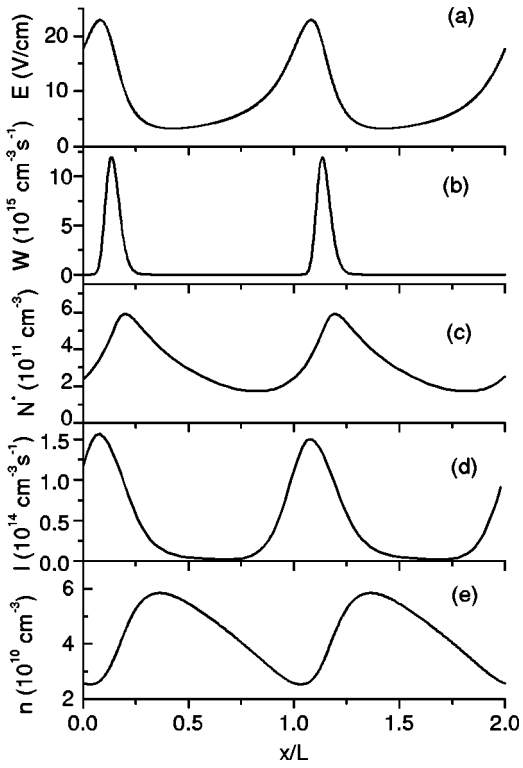

FIG. 10. The parameters of the nonlinear ionization wave calculated at $p=25$ Torr, $i=10$ mA in dependence on x. (a) Electric field; (b) excitation rate W; (c) excited atom density N^*; (d) ionization rate I; (e) electron density n.

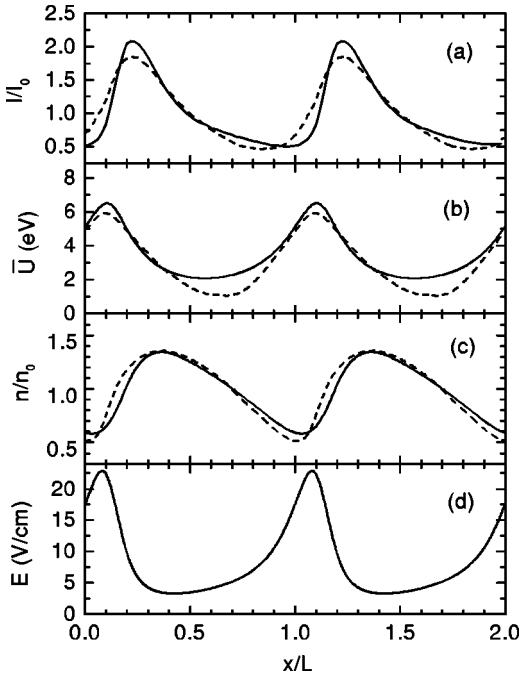

FIG. 11. The comparison of the theoretical (solid curve) and experimental (dashed curve) profiles of various plasma parameters in the ionization wave. $p=25$ Torr, $i=10$ mA, the wavelength $L=4.3$ cm. (a) Intensity of the radiation (dashed curve) and the stepwise excitation rate (solid curve); (b) electron mean energy; (c) electron density; (d) electric field.

It is interesting to compare the calculated and experimentally measured profiles of various plasma parameters. This comparison is performed in Fig. 11, where the solid curves correspond to the theory, and the dashed curves correspond to the experiment [5] ($p=25$ Torr). The experimental curve in the graph (a) corresponds to the radiation intensity distribution. In the graph (d) the calculated electric field is shown. Good agreement between the calculated and measured profiles of the atom radiation intensity, electron mean energy and density can be seen in this figure. An essential effect of nonlocality is the larger modulation of the electric field with the respect to the mean energy, that can be interpreted as the presence of electron thermoconductivity.

VIII. CONCLUSION

Description of the stratified discharge at intermediate pressures $p=10-40$ Torr and small currents $i<25$ mA requires a kinetic approach. In the present paper a one-dimensional kinetic model of ionization waves in a discharge under these conditions has been constructed, based on the coupled solution of the kinetic equation for electrons and the continuity equation for ions. The stepwise and associative ionization and the diffusion of the excited atoms mainly due to the axial transport of the resonance radiation have been taken into account. The linear theory of ionization waves under these conditions has been constructed, the dependence of growth rate and frequency of waves on the wavelength was found for various discharge conditions. The region where the growth rate is positive has been determined. The linear theory within the limits of its validity shows an upper bound for the existence of striations by pressure and a lower bound by current, which is in agreement with the experimental data. The dispersion relations calculated showed, that the group velocity of waves points against their phase velocity, that is a well-known feature of ionization waves.

A scheme of the solution of a nonlinear system of equations describing the ionization wave has been suggested. To obtain a unique solution, it is necessary to introduce an additional external parameter. The mean electric field was externally fixed as such a parameter.

A kinetic theory allows us to obtain the picture of the processes of excitation and ionization in different phases of the nonlinear wave. Comparison between theory and experiment showed good agreement.

ACKNOWLEDGMENTS

The work was partially supported by Deutsche Forschungsgemeinschaft (DFG) through Project SFB 198 ''Kinetics of partially ionized Plasma'' and Deutscher Akademischer Austauschdienst (DAAD). The work was supported by Grant No. 97-5.3-29 of the Russian Ministry of Education.

[1] S. Pfau, A. Rutscher, and K. Wojaczek, Contrib. Plasma Phys. **9**, 333 (1969).
[2] D. Venzke, E. Hayess, and K. Wojaczek, Contrib. Plasma Phys. **6**, 365 (1966).
[3] L.D. Tsendin, Zh. Tekh. Fiz. **39**, 1341 (1969).
[4] L.D. Tsendin, Sov. J. Plasma Phys. **8**, 96 (1982).
[5] Ju.B. Golubovskii, V.I. Kolobov, and I.E. Sulejmenov, Zh. Tekh. Fiz. **61**, 57 (1991).
[6] Ju.B. Golubovskii, V.I. Kolobov, and I.E. Sulejmenov, Zh. Tekh. Fiz. **61**, 62 (1991).
[7] Ju.B. Golubovskii, V.I. Kolobov, V.O. Nekuchaev, and I.E. Sulejmenov, Zh. Tekh. Fiz. **61**, 68 (1991).
[8] Yu.B. Golubovskii, V.A. Maiorov, I.A. Porokhova, and J. Behnke, J. Phys. D **32**, 1391 (1999).
[9] I.E. Sulejmenov, Dissertation, Leningrad State University, 1989.
[10] L.D. Tsendin and Yu.B. Golubovskii, J. Tech. Phys. **47**, 1839 (1977).
[11] F. Sigeneger and R. Winkler, Contrib. Plasma Phys. **36**, 551 (1996).
[12] F. Sigeneger, Yu.B. Golubovskii, I.A. Porokhova, and R. Winkler, Plasma Chem. Plasma Process. **18**, 153 (1998).
[13] Yu.B. Golubovskii, R.V. Kozakov, V.A. Maiorov, J. Behnke, and J.F. Behnke, Phys. Rev. E **62**, 2707 (2000).
[14] L.M. Biberman, Zh. Eksp. Teor. Fiz. **17**, 416 (1947).
[15] T. Holstein, Phys. Rev. **72**, 1212 (1947); **83**, 1159 (1951).
[16] Ju.B. Golubovskii, V.M. Zakharova, Ju.M. Kagan, and R.I. Lyaguschenko, Opt. Spectrosc. **40**, 971 (1976).
[17] L.A. Vainstein, I.I. Sobelman, and E.A. Yukov, *Cross Sections of Excitation of Atoms and Ions by Electrons* (Nauka, Moscow, 1973) (in Russian).
[18] *Physical Values, Reference Book*, edited by I.S. Grigorjev and E.Z. Mejlikhov (Energoatomizdat, Moscow, 1991) (in Russian).